

Dedicated to the memory of Prof. dr. Ioan Silaghi-Dumitrescu marking 60 years from his birth

BEHAVIOR OF MIXED DMPC-CHOLESTEROL MONOLAYERS AT THE AIR/WATER INTERFACE

AURORA MOCANU*, ROXANA-DIANA PAȘCA, OSSY HOROVITZ,
MARIA TOMOAIA-COTISEL

ABSTRACT. The phase behaviour of cholesterol (CHO) and dimyristoyl phosphatidyl choline (DMPC) monolayers at the air/water interface was investigated by surface pressure measurements using Langmuir technique. Compression isotherms and isobars as functions of composition were represented, and the surface compressibility modulus was calculated, in order to characterize the physical states of the monolayers. At a constant lateral surface pressure, the monolayers were transferred by Langmuir-Blodgett technique (LBT) from air-water interface on solid supports and further studied by atomic force microscopy (AFM). This study shows that the strong interactions between DMPC and CHO lead to well defined two-dimensional nanostructures, which can have practical applications for biosensors fabrication. Also, this type of nanostructures seems plausible to occur in natural membranes and thus, can influence the protein distribution and protein function *in vivo*.

Keywords: *cholesterol, DMPC, monolayers, Langmuir-Blodgett technique, atomic force microscopy*

INTRODUCTION

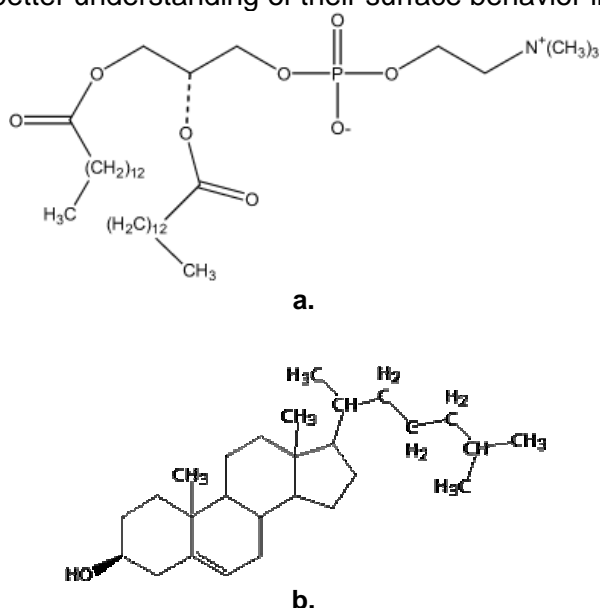
Phospholipids and cholesterol are the primary constituents of vertebrate cell membranes [1, 2] and their interaction is important for the membrane organization and properties [3-5]. Possible interactions are hydrogen bonds between the cholesterol OH-group and carbonylic oxygen atoms of the phospholipid DMPC (Scheme 1) and van der Waals forces [6].

An approach to the understanding of these interactions is the investigation of the organization of such biomolecules at the air/aqueous solution interfaces in the two-dimensional monomolecular layers, at controlled lateral surface pressures. These monolayers are realized by spreading and compressing the biomolecules at the air/water interface [7-9]. Dimyristoyl

* *Babeș-Bolyai University, Faculty of Chemistry and Chemical Engineering, Arany Janos 11, 400028 Cluj-Napoca, Romania, mcotisel@chem.ubbcluj.ro*

phosphatidyl choline (DMPC) is a typical biomolecule forming highly ordered monolayers [10-12]. The DMPC molecules can be spread, compressed and oriented at the air/water interface at various lateral surface pressures to form DMPC monolayers of close-packed polar groups within the interfacial water having the hydrocarbon chains oriented into the air phase. The interaction of phospholipids with sterols was studied both in films at the air/water interface [5, 6, 13-16] and on solid support, by AFM techniques [17, 18].

In the present paper, we have chosen cholesterol (CHO) and DMPC (Scheme 1) to be investigated in monolayers, which are considered as membrane models, for a better understanding of their surface behavior in mixed films.



Scheme 1. Chemical structures of DMPC (a) and cholesterol (b).

RESULTS AND DISCUSSION

The *compression isotherms* measured for DMPC, cholesterol and their mixtures at different ratios are represented as surface pressure, π , *versus* area per molecule, A (Fig. 1). Surface pressure is defined as the difference between the surface tension at the air/water interface, σ_o , and the surface tension, σ , at the same interface in the presence of the investigated monolayer:

$$\pi = \sigma_o - \sigma \quad (1)$$

The mole fractions of cholesterol (x_{CHO}) in the mixed monolayers varied from 0.1 to 0.9 (step value 0.1). It is evident that all compression isotherms are shifted towards left (smaller areas per molecule) with increasing x_{CHO} values, *i.e.* a condensing effect of cholesterol is manifested.

BEHAVIOR OF MIXED DMPC-CHOLESTEROL MONOLAYERS AT THE AIR/WATER INTERFACE

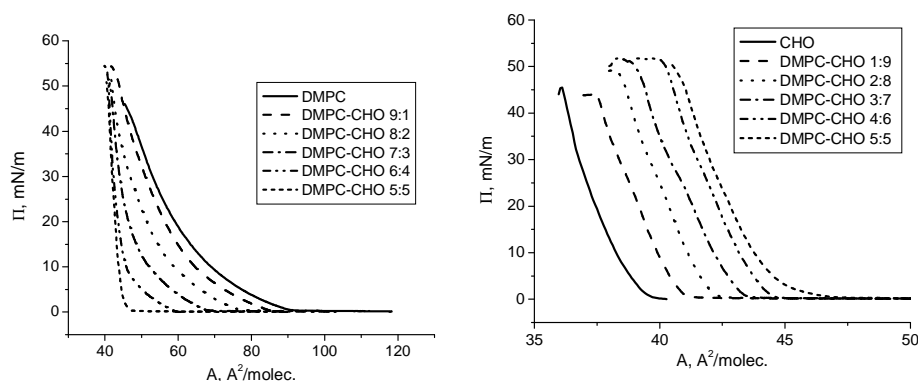


Figure 1. Representative compression isotherms for DMPC and DMPC-CHO mixed monolayers with $x_{\text{CHO}} \leq 0.5$ (a), and for CHO and DMPC-CHO mixed monolayers with $x_{\text{CHO}} \geq 0.5$ (b).

The differences in the collapse pressures (the highest lateral surface pressure for monolayer stability) for the various monolayers are also visible in these isotherms. While for the pure DMPC and CHO the values are the lowest (about 46 mN/m for DMPC, respectively 42 mN/m for CHO), the mixed monolayers present higher collapse pressures.

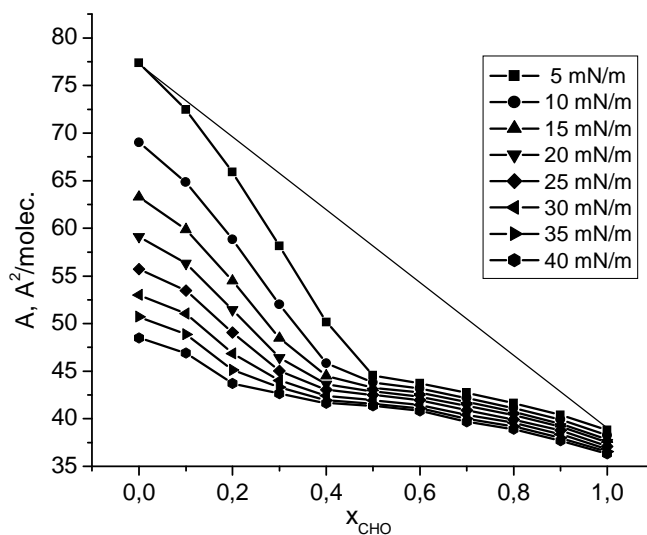


Figure 2. Mean molecular areas vs. cholesterol mole fractions in DMPC-CHO mixed monolayers at the surface pressures given in the inset.

A proof for the condensing effect of cholesterol in the mixed monolayers is given by the representation of mean areas per molecule, A , against the mixture composition, x_{CHO} , at constant values of the surface pressure, π . Such *isobars* are given in Fig. 2 for π -values from 5 up to 40 mN/m. This condensing effect, i.e. negative deviations from the mixing rule, represented by a straight line connecting the points for pure components (as the solid line given in Fig. 2 for $\pi = 5$ mN/m), is most pronounced for small values of the surface pressure, and it is maintained even with the highest lateral surface pressures.

This condensing effect of cholesterol, and therefore the higher packing density of mixed DMPC-CHO monolayers, can be ascribed to the attracting van der Waals forces and the hydrogen bondings between the phospholipids and cholesterol, stabilizing these mixed structures [13, 19-21] and inducing a chain ordering.

Isothermal compressibility of a monolayer is defined by:

$$C_s = -\frac{1}{A} \left(\frac{\partial A}{\partial \pi} \right)_T \quad (2)$$

Its reciprocal value, the surface compressibility modulus:

$$C_s^{-1} = -A \left(\frac{\partial \pi}{\partial A} \right)_T \quad (2a) \text{ the surface correspondent of the bulk modulus,}$$

$$K = -V \left(\frac{\partial p}{\partial V} \right)_T, \text{ is a measure of the interfacial elasticity and a characteristic}$$

for the variations in the physical state of the monolayers. The isothermal compressibility was calculated from the compression isotherms $\pi = f(A)_T$ in Fig. 1, by graphical derivation. Representations of surface pressures against C_s^{-1} values are given in Fig. 3.

In each case, the values of C_s^{-1} are roughly growing with increasing surface pressure, and reach a maximum for a surface pressure corresponding to the high packing in the monolayers before collapse. DMPC and mixed DMPC-CHO monolayers for $x_{\text{CHO}} \leq 0.2$ present the lowest and cholesterol (at least for high π -values) the highest C_s^{-1} values for the same surface pressure, while mixed monolayers show intermediate values. For cholesterol mole fractions above 0.5 the differences between mixed layers and pure cholesterol are diminished.

This surface compressibility modulus C_s^{-1} , is considered to be an indicator for the physical state of the monomolecular film [22]. When these values pass beyond 100 mN/m, the layer should attain the liquid-condensed (LC) state, whereas values above 250 mN/m suggest the presence of the solid state, implying a close packing of the hydrocarbon chains [6]. Applying

this criterion, all the mixed DMPC-CHO monolayers can pass by compression in the LC state, and even in the solid state, for various compositions with a higher cholesterol content ($x_{\text{CHO}} \geq 0.4$).

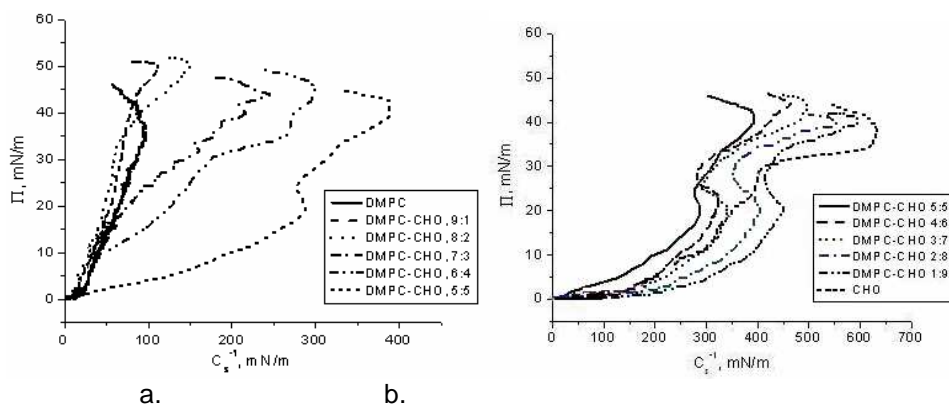


Figure 3. Surface pressure *versus* reciprocal isothermal compressibility for DMPC and DMPC-CHO mixed monolayers with $x_{\text{CHO}} \leq 0.5$ (a), and for CHO and DMPC-CHO mixed monolayers with $x_{\text{CHO}} \geq 0.5$ (b).

A representation of the surface pressures at which film collapse occurs, as seen in the compressibility isotherms (Fig. 1), against the cholesterol content of the DMPC-CHO mixtures (Fig. 4) shows a maximum for cholesterol mole fractions between 0.4 and 0.5, thus the most stable monolayers are obtained for these compositions.

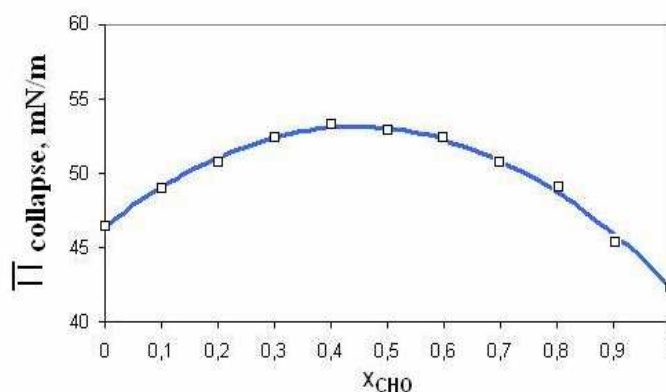


Figure 4. Surface pressures at film collapse *versus* cholesterol content in binary DMPC-CHO mixed monolayers.

AFM observations were used to complete the picture of DMPC, CHO and mixed DMPC-CHO layers near collapse pressure, transferred on glass surface. Representative AFM results are shown for pure DMPC film, (Fig. 5), pure cholesterol film (Fig. 6) and for one of the DMPC-CHO mixed monolayers, corresponding to a cholesterol mole fraction $x_{\text{CHO}} = 0.8$ (Fig. 7).

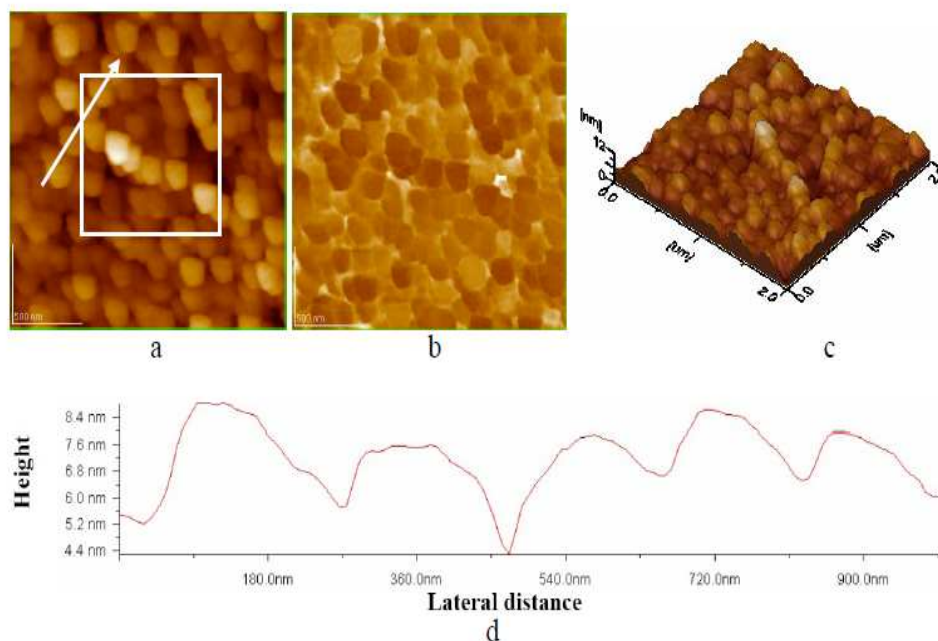


Figure 5. AFM images of DMPC film on optical polished glass near the collapse ($\pi_{\text{collapse}} = 46 \text{ mN/m}$). Scanned area $2 \mu\text{m} \times 2 \mu\text{m}$. a) 2D- topography; b) phase image; c) 3D-topography; d) profile of the cross-section along the arrow in panel a.

The 2D- and 3D-topography images (Fig. 5-7a and c) reveal nanostructures of high domains, up to 12 nm for DMPC (Fig. 5c) and the mixed layer (Fig. 7c) and to 10 nm for cholesterol (Fig. 6c). Most of these structures present an apparent height, as seen in the profiles of cross-sections, of about 8 or 9 nm for pure DMPC (Fig. 5 d) and the mixed film (Fig. 7d) and 5 – 6 nm for the cholesterol film (Fig. 6d). The phase (Fig. 5b, 6b) and the amplitude (Fig. 7b) images appear to be complementary to the topographic ones, showing the structural features of the monolayers. The size of the domains appears to be up to about 200 nm (Figs. 5d-7d).

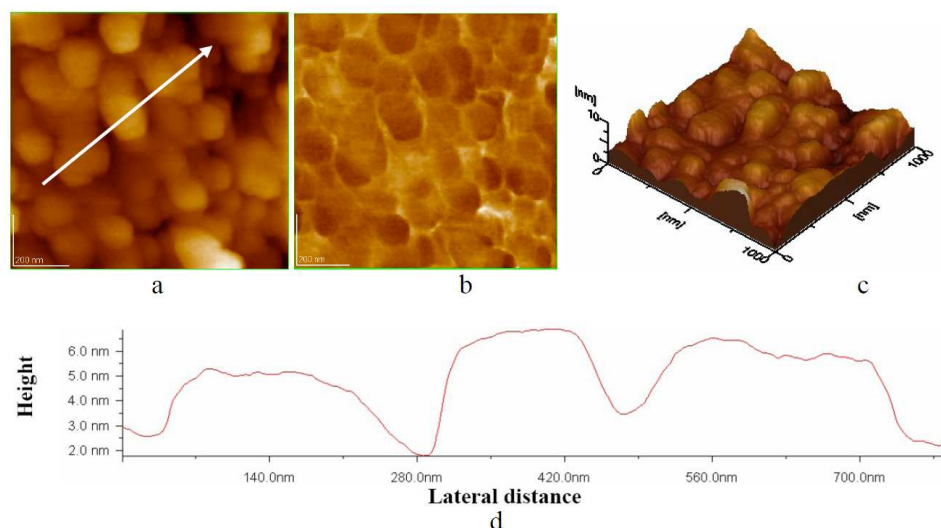


Figure 6. AFM images of cholesterol film on optical polished glass at collapse ($\pi_{\text{collapse}} = 42 \text{ mN/m}$). Scanned area $1 \mu\text{m} \times 1 \mu\text{m}$. a) 2D- topography; b) phase image; c) 3D-topography; d) profile of the cross-section along the arrow in panel a.

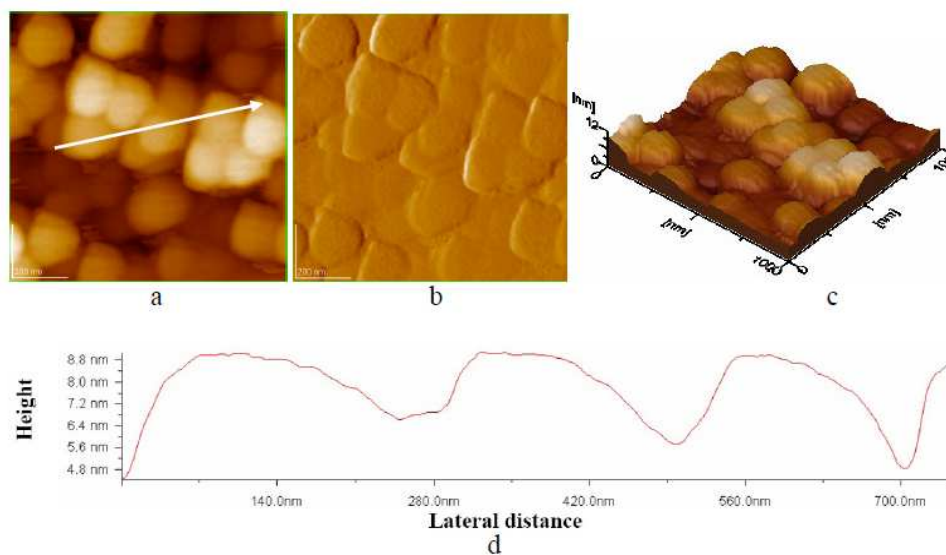


Figure 7. AFM images of a mixed DMPC-cholesterol film ($x_{\text{CHO}} = 0.8$) transferred on optical polished glass at $\pi_{\text{collapse}} = 50 \text{ mN/m}$. Scanned area $1 \mu\text{m} \times 1 \mu\text{m}$. a) 2D- topography; b) amplitude image; c) 3D-topography; d) profile of the cross-section along the arrow in panel a.

CONCLUSIONS

Cholesterol, DMPC and their mixtures containing the two biomolecules in ratios from 9:1 to 1:9 were studied as monolayers at the air/water interface and as Langmuir-Blodgett films transferred on solid glass support. These films are important as membrane models, and their investigation is a step towards the understanding of membrane structure and properties.

From the measured compression isotherms (surface pressure vs. molecular area) and isobars (molecular area vs. composition at constant surface pressure), the condensing effect of cholesterol in the mixed films with DMPC is clearly evidenced. It results from the chain ordering and the stabilization of the mixed structures, due to hydrogen bonds and van der Waals attractions between cholesterol and DMPC molecules, resulting in a higher packing density. The increased stability for DMPC-CHO mixed films at nearly equimolar ratio is also evidenced by regularities found in the collapse pressure of these films.

From the surface compressibility module of the monolayers, obtained by derivation of the compression isotherms, the physical states of the films (liquid-condensed state and solid state) could be assigned

AFM images of the films transferred on solid surface near their collapse pressure revealed the formation of characteristic nanostructured domains.

EXPERIMENTAL SECTION

1,2-Dimyristoyl-*sn*-glycero-3-phosphocholine (DMPC) and β -cholesterol (CHO) were purchased from Sigma (Saint Louis, USA) and used without further purification. Benzene (>99.8%) was a product of Lach-Ner (Czech Republic), hexane (>99%) and ethanol (>99.5%) were purchased from Merck (Germany). All organic solvents used were analytical grade reagents. Ultra pure water with a resistivity greater than 18 M Ω cm, obtained from an Elga apparatus was used in all experiments. Its pH was 5.5 and its surface tension was superior to 71.8 mN/m at 25°C. All glass ware was cleaned with sulfochromic mixture and then abundantly rinsed with the distilled water. Optically polished glass was used as solid support in the deposition process, after cleaning with sulfochromic mixture followed by rinsing with deionized water.

Surface pressure vs. area per molecule isotherms were recorded using KSV LB Standard Trough (KSV Ltd., Finland) controlled by KSV-5000 software and equipped with two movable barriers, a Wilhelmy balance, and a dipper for monolayers transfer from air/water interface to solid support. A Teflon trough with effective area of 765 cm² was used in all experiments; the volume of the subphase was 1500 cm³. Deionized highly purified water was used as the subphase. Before each measurement, the subphase surface was cleaned by sweeping and suction processes.

The spreading solutions used were made in benzene (CHO, ca. 1 mg/ml), ethanol/hexane mixture (2:98, v/v) for DMPC, and by mixing DMPC and CHO at different molar ratios (concentration of mixed solutions of about 1 $\mu\text{mol/ml}$). The organic solutions were spread with a Hamilton syringe. After spreading, the solution was left for 10 min for solvent evaporation. The compression of the monolayer was performed at a rate of 15 mm/min for CHO monolayer, 10 mm/min for DMPC monolayer and 15 mm/min for DMPC:CHO mixtures. All isotherms were recorded upon symmetric compression of the monolayer. For each monolayer composition, measurements were repeated at least three times.

AFM measurements were made on Langmuir-Blodgett (LB) films of DMPC in the absence and in the presence of CHO and on CHO pure films on optically polished glass supports. The vertical LB deposition method was used, at constant lateral surface pressures, near the collapse pressure of the individual monolayer. The measurements were conducted in tapping mode on the scanning probe microscope (AFM-JEOL 4210, Japan). The calibration of the AFM scanner was checked by imaging freshly cleaved highly oriented pyrolytic graphite (HOPG) and muscovite mica samples. Non-contact conical shaped tips of silicon nitride coated with aluminum were used. The tip was on a cantilever with a resonant frequency in the range of 200 - 300 kHz and with a spring constant of 17.5 N/m. We used low scan rates of 1 Hz and high scan rates in the range of 20-30 Hz to detect noise artefacts. The scan angle was also changed in different directions to observe real images from those corresponding to noise. AFM observations are repeated on different areas from 10 $\mu\text{m} \times 10 \mu\text{m}$ to 0.5 $\mu\text{m} \times 0.5 \mu\text{m}$ of the same LB film. The AFM images were obtained from at least three macroscopically separated areas on each LB film. All images were processed using the standard procedures for AFM. The widths and the thickness variations of the domains were estimated from AFM topographic images and cross-section profiles. AFM images consist of multiple scans displaced laterally from each other in y direction with 256 x 256 pixels. Low pass filtering was performed to remove the statistical noise without to loose the features of the sample. All AFM experiments were carried out under ambient laboratory conditions (about 20°C) as previously reported [23-26].

ACKNOWLEDGMENTS

One of us (Roxana-Diana Pașca) has received financial support for this study from the *Babes-Bolyai University of Cluj-Napoca, Romania* (Programme No. 32/2009).

REFERENCES

1. W. R. Nes, *Lipids*, **1974**, 9, 596.
2. J. Henriksen, A. C. Rowat, E. Brief, Y. W. Hsueh, J. L. Thewalt, M. J. Zuckermann, J. H. Ipsen, *Biophysical Journal*, **2006**, 90, 1639.
3. J. Pencer, M. P. Nieh, T. A. Harroun, S. Krueger, C. Adams, J. Katsaras, *Biochimica Biophysica Acta*, **2005**, 1720, 84.
4. J. Henriksen, J., A. C. Rowat, J. H. Ipsen, *European Biophysics Journal*, **2004**, 33, 732.
5. M. D Ali, K. H. Cheng, J. Huang, *Proceedings of the Natural Academy of Sciences USA*, **2007**, 104, 5372.
6. K. Sabatini, J.-P. Mattila, P. K. J. Kinnunen, *Biophysical Journal*, **2008**, 95, 2340.
7. O. Albrecht, H. Gruler, E. Sackmann, *Journal of Colloid and Interface Science*, **1981**, 79, 319.
8. V. Vogel, D. Mobius, *Journal of Colloid and Interface Science*, **1988**, 126, 408.9.
M. Tomoaia-Cotisel, Gh. Tomoaia, V. D. Pop, A. Mocanu, O. Cozar, N. Apetroaei, Gh. Popa, *Revue Roumaine de Chimie*, **2005**, 50, 471.
10. L. Berthelot, V. Rosilio, M. L. Costa, S. Chierici, G. Albrecht, P. Boullanger, A. Baszkin, *Colloids and Surfaces B: Biointerfaces*, **1998**, 11, 239.
11. C. A. S. Andrade, N. S. Santos-Magalhães, C. P. de Melo, *Journal of Colloid and Interface Science*, **2006**, 298, 145.
12. D. Matyszevska, R. Bilewicz, *Colloids and Surfaces A: Physicochemical and Engineering Aspects*, **2008**, 321, 11.
13. P. Dynarowicz-Latka, K. Hac-Wydro, *Colloid Surfaces B: Biointerfaces*, **2004**, 37, 21.
14. Y. Tagami, T. Narita, H. Ikigai, Y. Oishi, *Colloids and Surfaces A: Physicochemical and Engineering Aspects*, **2009**, 347, 225.
15. B. Korchowiec, M. Paluch, Y. Corvis, E. Rogalska, *Chemistry and Physics of Lipids*, **2006**, 144, 127.
16. Y. Su, Q. Li, L. Chen, Z. Yu, *Colloids and Surfaces A: Physicochemical and Engineering Aspects*, **2007**, 293, 123.
17. Y. Tagami, H. Ikigai, Y. Oishi, *Colloids and Surfaces A: Physicochemical and Engineering Aspects*, **2006**, 284, 475.
18. C. Yuan, L. J. Johnston, *Biophysical Journal*, **2001**, 81, 1059.
19. Yeagle, P. L., *Biochimica et Biophysica Acta*, **1985**, 822, 267.
20. E. E. Berring, K. Borrenpohl, S. J. Fliesler, A. Barnoski Serfis, *Chemistry and Physics of Lipids*, **2005**, 136, 1.
21. K. Kim, C. Kim, Y. Byun, *Langmuir*, **2001**, 17, 5066.
22. J. T. Davies, E. K. Rideal, "Interfacial Phenomena", 2nd ed., Academic Press, New York, **1963**.
23. M. Tomoaia-Cotisel, A. Tomoaia-Cotisel, T. Yupsanis, G. Tomoaia, I. Balea, A. Mocanu, C. Racz, *Revue Roumaine de Chimie*, **2006**, 51, 1181.
24. O. Horovitz, G. Tomoaia, A. Mocanu, T. Yupsanis, M. Tomoaia-Cotisel, *Gold Bulletin*, **2007**, 40, 213.
25. M. Tomoaia-Cotisel, A. Mocanu, *Revista de Chimie (Bucharest)*, **2008**, 59, 1230.
26. A. Mocanu, I. Cernica, G. Tomoaia, L. D. Bobos, O. Horovitz, M. Tomoaia-Cotisel, *Colloids and Surfaces A: Physicochemical and Engineering Aspects*, **2009**, 338, 93.